Manipulation of dietary amino acids prevents and reverses obesity in mice through multiple mechanisms that modulate energy homeostasis

Chiara Ruocco,[1] Maurizio Ragni,[1] Fabio Rossi,[1] Pierluigi Carullo,[2] Veronica Ghini,[3] Fabiana Piscitelli,[4] Adele Cutignano,[4] Emiliano Manzo,[4] Rafael Maciel Ioris,[5,6] Franck Bontems,[5,6] Laura Tedesco,[1] Carolina Greco,[2] Annachiara Pino,[7] Ilenia Severi,[8] Dianxin Liu,[9] Ryan P. Ceddia,[9] Luisa Ponzoni,[1,10] Leonardo Tenori,[11,12] Lisa Rizzetto,[13] Matthias Scholz,[13] Kieran Tuohy,[13] Francesco Bifari,[1,14] Vincenzo Di Marzo,[4] Claudio Luchinat,[3,15] Michele O. Carruba,[1] Saverio Cinti,[8] Ilaria Decimo,[7] Gianluigi Condorelli,[2] Roberto Coppari,[5,6] Sheila Collins,[9] Alessandra Valerio,[16] and Enzo Nisoli[1]

[1]Center for Study and Research on Obesity, Department of Biomedical Technology and Translational Medicine, University of Milan, Milan, Italy; [2]Humanitas University, Rozzano, Italy; [3]Interuniversity Consortium for Magnetic Resonance, Sesto Fiorentino, Italy; [4]Institute of Biomolecular Chemistry, Consiglio Nazionale delle Ricerche, Pozzuoli, Italy; [5]Department of Cell Physiology and Metabolism, University of Geneva, Geneva, Switzerland; [6]Diabetes Center of the Faculty of Medicine, University of Geneva, Geneva, Switzerland; [7]Department of Diagnostics and Public Health, University of Verona, Verona, Italy; [8]Department of Experimental and Clinical Medicine, University of Ancona (Politecnica delle Marche), Ancona, Italy; [9]Division of Cardiovascular Medicine, Department of Medicine, Vanderbilt University Medical Center, Nashville, Tennessee, USA; [10]Umberto Veronesi Foundation, Milan, Italy; [11]FiorGen Foundation, Sesto Fiorentino, Italy; [12]Center of Magnetic Resonance, University of

Florence, Sesto Fiorentino, Italy; [13]Department of Food Quality and Nutrition, Research and Innovation Center, Fondazione Edmund Mach, San Michele all'Adige, Italy; [14]Laboratory of Cell Metabolism and Regenerative Medicine, Department of Medical Biotechnology and Translational Medicine, University of Milan, Milan, Italy; [15]Department of Experimental and Clinical Medicine, University of Florence, Florence, Italy; [16]Department of Molecular and Translational Medicine, Brescia University, Brescia, Italy

Corresponding author:

Enzo Nisoli

Department of Biomedical Technology and Translational Medicine

University of Milan, Milan – 20129 (Italy)

Telephone number: +30 02 50316956; Email: enzo.nisoli@unimi.it

C.R. and M.R. contributed equally to this work.

Short title: Dietary amino acids and energy metabolism

The manuscript contains: 6,689 words, 8 figures, 13 supplementary figures, and 10 supplementary tables.

Tweet:

A designer protein-deprived diet enriched in essential amino acids promotes brown fat thermogenesis, stimulates uncoupling protein 1-independent respiration in white fat, changes the gut microbiota composition and prevents and reverses obesity, extending healthspan.

Figure 3A best summarizes our article

Reduced activation of energy metabolism increases adiposity in humans and other mammals. Thus, exploring dietary and molecular mechanisms able to improve energy metabolism is of paramount medical importance, as such mechanisms can be leveraged as a therapy for obesity and related disorders. Here, we show that a designer protein-deprived diet enriched in free essential amino acids can i) promote the brown fat thermogenic program and fatty acid oxidation, ii) stimulate uncoupling protein 1 (UCP1)-independent respiration in subcutaneous white fat, iii) change the gut microbiota composition, and iv) prevent and reverse obesity and dysregulated glucose homeostasis in multiple mouse models, prolonging the healthy lifespan. These effects are independent of unbalanced amino acid ratio, energy consumption, and intestinal calorie absorption. A brown fat-specific activation of the mechanistic target of rapamycin complex 1 seems involved in the diet-induced beneficial effects, as also strengthened by *in vitro* experiments. Hence, our results suggest that brown and white fat may be targets of specific amino acids to control UCP1-dependent and -independent thermogenesis, thereby contributing to the improvement of metabolic health.

Although debatable, chronic consumption of diets with a high ratio of saturated to unsaturated fatty acids (SFA diets) increases body adiposity, impairs glucose homeostasis, raises the cardiovascular risk, and reduces the healthy disease-free lifespan in animals and humans (1,2). These diets negatively affect the proper secretion and action of key hormones—insulin, leptin, and adiponectin—underlying metabolic homeostasis and energy balance (3). The increased consumption of high-calorie, low-fiber diets has contributed significantly to the staggering rise in overweight, obesity, and type 2 diabetes prevalence in the past few decades (4). Likewise, high-protein diets have been advocated since the 1960s as a means of weight loss and to prevent obesity and its metabolic sequelae (5). However, the long-term safety of such diets has been recently questioned by increasing evidence of raised cardiovascular risk (6). Accordingly, great excitement was built by the demonstration that protein-restricted diets (7), or diets with lower concentrations of single or multiple essential amino acid (*e.g.*, leucine, methionine, or tryptophan; EAAs), were correlated to improved energy balance and decreased overweight or obesity, in mice and humans (8,9). In contrast, several studies have also shown the efficacy of central or peripheral supplementation of a single amino acid (*e.g.*, glycine, leucine, or tryptophan) in modulating energy metabolism and/or body weight (10,11). However, not all of these findings were confirmed by others (12).

To investigate these conflicting results, we conducted in-depth analyses on metabolic effects, in normal-weight and obese mice, caused by acute and chronic consumption of two customized diets. Specifically, the protein content (*i.e.*, casein) of the SFA diet (10 % fat) and high-fat diet (HFD, 60 % fat) was substituted with an original formula composed by EAAs (SFA-EAA and HFD-EAA) (for nutrient compositions see below). The EAA mixture was stoichiometrically similar to the formula we previously showed to promote mitochondrial biogenesis in skeletal and cardiac muscles of middle-aged mice and to ameliorate health, especially

in older adults, when consumed as a dietary supplement with drinking water (13,14). The metabolic effects of SFA-EAA and HFD-EAA diets were compared to those owed to two isocaloric, isolipidic, and isonitrogenous diets, identical to SFA or HFD diet except for casein replacement by the purified amino acid mixture designed on the amino acid profile of casein (SFA-CAA and HFD-CAA diets), in addition to those induced by a chow diet. In particular, drinking supplementation of the EAA mixture was found to prevent oxidative stress in metabolically active cells (14–16), ameliorating muscle and cognitive performance in diverse animal models and humans (17,18). Moreover, a relevant rejuvenation was observed in the gut microbiota of ageing mice supplemented with the EAA mixture (19). This observation seems to be of relevance because diet composition may affect energy balance also through intestinal microbiota. For example, dietary amino acid intake increases the relative abundance of *Bacteroidetes* (20), and EAA-derived short-chain fatty acids modulate the overall lipid balance and glucose metabolism (21). Also, the gut microbiota controls adiposity (22) and can activate adaptive thermogenesis in mice (23).

Adaptive thermogenesis refers to the generation of heat by the body in response to external stimuli (*e.g.*, cold temperature, ingestion of high-calorie foods). It includes shivering and non-shivering thermogenesis (NST) The activation of brown adipocytes, in brown adipose tissue (BAT), and beige adipocytes, in visceral and subcutaneous fat depots, contributes substantially to NST (24). These thermogenic adipocytes express uncoupling protein 1 (UCP1), a protein that uncouples respiration and leads to energy dissipation in the form of heat. Ablation of brown or beige adipocytes predisposes mice to develop obesity and type 2 diabetes (25,26), as does deletion of the *Ucp1* gene (27). Conversely, increasing the number or activity of thermogenic adipocytes protects against body weight gain and metabolic disease (28). Mechanistic target of rapamycin complex 1 (mTORC1) activation is required for BAT recruitment and metabolic adaptation to cold (29,30). Additional mechanisms activate thermogenesis in an UCP1-independent manner: the

glycerol phosphate shuttle, calcium-dependent ATP hydrolysis, and creatine-dependent substrate cycling (31–33). Also, *N*-acyl amino acids stimulate uncoupled mitochondrial respiration in white adipocytes, independently of UCP1, and their systemic administration activates the whole-body energy expenditure (34).

Here we show that almost complete substitution of the casein in standard rodent diets with a unique amino acid mixture modulated energy homeostasis in diet-induced obesity or a model of genetic obesity. Our results reveal multiple thermogenic mechanisms by which designer diets could be used to combat obesity and type 2 diabetes.

RESEARCH DESIGN AND METHODS

Animals, diets, and treatments

Male C57BL/6N mice (8 weeks old), from Charles River (Calco, Italy), were weight-matched and fed *ad libitum* for different periods of time with normal chow diet (CD: V1534-300, Ssniff Spezialdiäten GmbH, Soest, Germany), SFA diet (20 % protein – namely casein –, 70 % carbohydrate, and 10 % fat, half of which was lard (D12450H), HFD diet [20 % protein, 10 % carbohydrate, and 60 % fat (D12492)], or two isocaloric, isolipidic, and isonitrogenous diets, identical to SFA or HFD diet except for protein which was almost completely (93.5 %) replaced by defined free EAAs (SFA-EAA, D14032501 or HFD-EAA, D17073104) or a purified amino acid mixture designed on the amino acid profile of casein (SFA-CAA diet, A17092801, or HFD-CAA, A20040601) all from Research Diets Inc. (Brogaarden, Gentofte, Denmark) (Supplementary Table 1).

Body weight and food intake were recorded twice a week in mice housed individually (except for the survival study); A cohort of C57BL6/N (8 weeks old) and *ob*/*ob* (6 weeks old, C57BL/6J background) male mice were kept and examined at thermoneutrality (30 °C) for the entire treatment period. For norepinephrine (NE) turnover analysis mice fed for 6 weeks with SFA-CAA and SFA-EAA diets were i.p. treated with α-methyl-para-tyrosine (AMPT, Sigma Aldrich) at time 0 (300 mg/kg BW) and after 2 h (150 mg/kg BW). Mice were sacrificed after 4 h and NE content was determined on iBAT with the Noradrenaline High Sensitive ELISA kit (Diagnostika GMBH, Hamburg, Germany), following manufacturer's instructions. For selective inhibition of mTORC1, mice were i.p. injected with rapamycin (Rapa, 2.5 mg/kg body weight) or vehicle (Veh, 0.2 % carboxymethylcellulose, 0.25 % Tween 80 in sterile water) (all from Sigma Aldrich), 5 days per week for 6 weeks, starting with diets. All mice used have a C57BL/6N background, that does

not exhibit defects of insulin release and mitochondrial dysfunction relative to C57BL/6J mice (35). Body composition were determined using the EchoMRI-100 system (Houston, TX, USA) , as previously described (36). Tissue samples for molecular analysis were snap-frozen in liquid nitrogen and prepared as described below.. All animal procedures were conducted in accordance with the European Community Guidelines and those of the Italian Ministry of Health, complied with the National Animal Protection Guidelines.

Caloric absorption and gut motility

At the end of treatments, feces were collected from each mouse, and energy content was measured by calorimetric bomb analysis (LECO AC-350, Milan, Italy). To monitor gut motility, whole gut transit time was measured as described (37). As parameters of absorbent capacity and epithelial morphology, the villi length of jejunum from frozen sections of intestine was determined by the Nikon Lucia IMAGE (v. 4.61) image analysis software (37).

Glucose homeostasis and biochemical analysis

Glucose (GTT) and pyruvate (PTT) tolerance test were performed after overnight fasting by i.p. injection of glucose or pyruvic acid (each 1.5 g/kg body weight) (Sigma Aldrich). Insulin tolerance test (ITT) was performed after 4 h daytime fast, with 0.5 U/kg body weight insulin i.p. injection (Sigma Aldrich). Glucose levels were measured in tail-vein blood using a Glucometer MyStar Extra (Sanofi, Milan, Italy) and test strips, at different time points after bolus. Plasma biochemistry and thyroxine levels were provided by Charles River Laboratories Service (Charles River Clinical Pathology/Immunology Laboratories, Wilmington, MA, USA). Metabolites and hormones were measured by commercial kits (Supplementary Table 2). Mean lipid droplet density and area in

iBAT were measured by the Nikon Lucia IMAGE (v. 4.61) image analysis software and calculated in 25 brown adipocytes for each sample.

Behavioral tests

The social dominance tube test and the elevated plus-maze test were carried out with mice fed with SFA, SFA-CAA, and SFA-EAA diet for 20 months, as described (38). Spontaneous motor activity was evaluated using an activity cage (Ugo Basile, Varese, Italy) placed in a sound-attenuating room, while an object recognition test was conducted in an open plastic arena.

Indirect calorimetry, locomotor activity, and temperature measurements

Metabolic efficiency was calculated as the ratio between body weight gain and the total energy intake over five days, 2 or 6 weeks. For *in vivo* indirect calorimetry analysis, mice were transferred in a Phenomaster System (TSE Systems GmbH, Bad Homburg, Germany) 1 week before the study started for acclimatization, followed by three weeks of continued measurements, as previously described (36). Core body temperature was obtained with a rectal probe (Physitemp Instruments Inc., Clifton, NJ, USA). Shaved back temperature was measured to estimate the level of iBAT thermogenesis, by infrared thermography, with a thermo-electrically cooled Thermocam P25 (Flir Systems Inc., Wilsonville, OR, USA) (37). *In vivo* images were captured and analyzed using the Flir quick report software according to the manufacturer's specifications.

Mass spectrometry analysis

Plasma samples and iBAT were extracted from mice after night-feeding, and their amino acid content was quantitated using the ACCQ·Tag derivatization reagent provided by Waters Chromatography Europe BV (Etten-Leur, The Netherlands). All amino acids were acquired in

positive polarity, in both TOF MS and Product Ion mode, according to the m/z values reported in Supplementary Table 3.

Fecal microbiota analysis

Fresh feces were collected, immediately frozen and stored. After extraction of total DNA (FastDNA™ SPIN Kit for Feces, MP Biomedicals, USA), 16S rRNA sequencing analysis was performed. Alpha and beta-diversity were determined using Quantitative Insight into Microbial Ecology (QIIME). Data are accessible at the European Nucleotide Archive with the accession number PRJEB25686.

Primary brown adipocytes

Mouse brown fat precursor cells were enzymatically isolated from iBAT of C57BL/6N male mice and differentiated in culture for nine days as previously described (39). Primary brown adipocytes maintained in amino-acid free DMEM (US Biological Life Science, DBA, Milan, Italy) for 16 h, were pretreated with rapamycin (1.0 nM) or vehicle (DMSO, Sigma Aldrich) for 1 h and subsequently supplemented for further 24 h with one of two different amino acid combinations, precisely reproducing the iBAT aminograms resulting from consumption of SFA-CAA or SFA-EAA diet (Supplementary Table 4). Cellular oxygen consumption rates (OCRs) were determined using a Seahorse XF24 Extracellular Flux Analyzer (Agilent, Santa Clara, CA, USA). Before analysis, the culture medium was changed to respiration medium. After basal respiration, uncoupled and maximal respiration was determined following the addition of oligomycin (1 μM) and subsequently carbonyl cyanide-4-trifluoromethoxy phenylhydrazone (FCCP, 0.2 μM). Rotenone (3 μM) was used to abolish mitochondrial respiration. All reagents were purchased from Sigma-Aldrich.

Gene expression and mitochondrial physiology

Quantitative RT-PCR reactions were performed as described (32) and run with the iQSybrGreenI SuperMix (Bio-Rad; Segrate, Italy) on an iCycler iQ Real-Time PCR detection system (Bio-Rad). mtDNA was amplified using primers specific for the mitochondrial cytochrome b gene and normalized to genomic DNA (gDNA). Primers were designed using Primer3 (version 0.4.0) software and are shown in Supplementary Table 5. Immunoblot analysis was performed as described (32). The antibodies (each at 1:1,000 dilution) are reported in Supplementary Table 2. Citrate synthase activity was measured spectrophotometrically in gastrocnemius as described (32). Carnitine palmitoyltransferase I (CPT1) activity was measured spectrophotometrically in iBAT mitochondria, as previously described (40). Electron microscopy analysis was conducted in thin sections of iBAT stained with lead citrate and examined with a CM10 transmission electron microscope (Philips, Eindhoven, Netherlands). Mitochondrial OCR was measured in a gas-tight vessel equipped with a Clark-type oxygen electrode (Rank Brothers Ltd., Cambridge, UK). Briefly, mitochondria from iWAT and iBAT were isolated, and respiration was measured as described (34). Liver and gastrocnemius mitochondria respiration was assessed in 137 mM KCl, 10 mM HEPES pH 7.2, 2.5 mM $MgCl_2$, 0.1% BSA, and 2 mM K_2HPO_4. iBAT OCR was measured by sequential addition of 2.5 mM malate, 30 μM palmitoyl-CoA plus 5 mM carnitine, 2 mM GDP, 100 μM ADP, 0.01 mg/mL oligomycin, and FCCP (500 nM), all from Sigma Aldrich. UCP1-dependent respiration was calculated as the amount of ADP-independent respiration that was inhibited by GDP, as described (24). For iWAT, liver, and gastrocnemius the same substrates, except GDP, were used.

N-acyl amino acid and acylcarnitine measurements by LC-HRMS

N-acyl amino acids were synthesized and measured, as previously described (34). Targeted quantitative analysis was carried out on extracted ion chromatograms corresponding to the molecular ion m/z values $[M-H]^-$ for *N*-acyl amino acid and $[M+H]^+$ for long-chain acylcarnitines (LCACs). Quantitation of *N*-acyl amino acid and LCACs was performed by integrating the area under the peak of each natural compound and normalizing to the corresponding internal standard area value.

Statistical analyses

Statistical analysis was performed by unpaired Student's t-test for two-group analysis or one-way ANOVA with Tukey correction or two-way ANOVA with Bonferroni correction for multiple group comparisons. Kaplan–Meier survival curves were created with the log-rank test equal to the Mantel–Haenszel test. A P value < 0.05 was considered statistically significant. Correlations were determined by nonparametric Spearman correlation test using the computer program GraphPad Prism (version 6.04).

Data and Resource Availability

The data sets generated and analyzed during the current study are available from the corresponding author upon reasonable request.

RESULTS

Effects on body weight, body composition, and adipose tissue

The subacute (6-week) and chronic (80-week) consumption of SFA diet increased body weight and adiposity independently of body length and lean mass, with higher circulating leptin levels compared to mice fed a chow diet (Fig. 1*A*-*D* and Supplementary Fig. 1*A*). Feeding mice with SFA-EAA diet prevented obesity development, maintaining lower fat mass and circulating leptin levels, without affecting lean mass or the normal growth of mice (Fig. 1*A*-*D* and Supplementary Fig. 1*A* and *B*). Notably, after 44 weeks mice fed with SFA-EAA diet weighed less than mice fed with a chow diet, with reduced body weight and adiposity until sacrifice (Fig. 1*A* and *C*). In addition to this preventive anti-obesity action, our designer diet exerted a potent therapeutic effect in which mouse body weight dropped after the switch from the SFA diet to the SFA-EAA diet (Fig. 1*A*). Body weight of the SFA-fed mice that were switched to the SFA-EAA diet indeed decreased to the level of chow-fed mice in ~2.5 months (Fig. 1*A*). Notably, the specific EAA substitution for casein entirely prevented the body weight gain, fat mass accumulation, and adiposity also induced by HFD consumption (Supplementary Fig. 2*A*-*C*). Similarly, the HFD-EAA diet strongly reduced body weight in already obese mice (Supplementary Fig. 2*A*, left). By contrast, both CAA-substituted diets were unable to prevent the obesity development or reduce body weight in already obese animals (Fig. 1*A*-*D*, Supplementary Fig. 2*A*-*C*).

The experiments mentioned above were conducted at room temperature (*i.e.*, at ~ 22 °C), a condition known to cause an increase of food intake and metabolism in small rodents to maintain body temperature (41). Thus, to determine the contribution of environmental thermal stress, we tested the metabolic effect of our engineered diets in C57BL6/N and leptin-deficient *ob*/*ob* mice

at thermoneutrality (41). Our additional experiments confirmed the heathy effects of SFA-EAA diet under this condition (Supplementary Fig. 2*D*).

Effects on glucose homeostasis and adipokines

Mice fed with the SFA-EAA diet for either six weeks or 11 months at room temperature had improved glucose and pyruvate tolerance and insulin-induced glycemia-lowering response compared to those of mice fed with either the SFA or SFA-CAA diets (Fig. 1*F* and Supplementary Fig. 1*C*-*G*). Fasting blood glucose and insulin concentrations did not differ among mice fed with different diets (Supplementary Table 6). These phenotypes were also observed when the SFA-EAA diet was consumed at 30 °C in C57BL6/N (Fig. 1*G*) and *ob*/*ob* mice (Supplementary Fig. 2*E*), and in HFD-EAA-fed mice at room temperature (Supplementary Fig. 2*F* and *G*). These results were confirmed by the circulating levels of adiponectin (89 ± 15 % higher, $P < 0.05$) in mice fed with the SFA-EAA diet compared to mice fed with the SFA-CAA diet (Fig. 1*H*). Accordingly to its inverse association to adiponectin in type 2 diabetes (42), insulin-like growth factor 1 (IGF1) was reduced in plasma of SFA-EAA-fed mice as compared to SFA-CAA-fed animals (Fig. 1*I*).

Effects on the whole body and hepatic lipid metabolism

Management of dyslipidemia is a crucial approach to reduce cardiovascular risk in obese and diabetic patients. Plasma nonesterified fatty acid (NEFA) levels, higher after consumption of the obesogenic diets (SFA and HFD), were reduced in both SFA-EAA- and HFD-EAA-fed mice, to values observed in mice on chow diet (Supplementary Fig. 3*A*). Total cholesterol plasma levels were increased in HFD-treated mice, whereas circulating triglycerides were similar between groups (Supplementary Fig. 3*B* and *C*). Unlike HFD-CAA, the HFD-EAA diet statistically prevented cholesterol increase induced by HFD (Supplementary Fig. 3*B*). These systemic effects

were mirrored by the ability of both SFA-EAA and HFD-EAA diet to prevent the increased NEFA, triglyceride and cholesterol levels of the liver in SFA- and HFD-fed mice (Supplementary Fig. 3*D-F*). Accordingly, macroscopic liver appearance and liver weight confirmed these results (Supplementary Fig. 3*G* and *H*). Mitochondrial respiration with palmitoyl carnitine as substrate suggested that EAA substitution promoted fat oxidation in the liver of both SFA- and HFD-fed mice (Supplementary Fig. 3*I*). Both CAA-substituted diets were ineffective.

Plasma amino acids

Next, we evaluated the effects of diets on amino acids in plasma. Alanine, glutamine, lysine, and threonine were higher with both EAA- and CAA-substituted diets than with SFA diet, though threonine was much more increased in SFA-EAA- than SFA-CAA-fed mice (Supplementary Fig. 4). In addition to threonine, the SFA-EAA diet increased histidine and valine levels over both SFA and SFA-CAA diet (Supplementary Fig. 4). Glycine and serine levels, which were markedly augmented in the SFA-CAA mice, with the SFA-EAA diet were similar to those observed in the SFA-fed mice (Supplementary Fig. 4). Notably, the levels of valine, histidine, and threonine were inversely correlated to the body weight and adiposity, isoleucine was inversely correlated to the body weight but not adiposity, while leucine was correlated with neither (Supplementary Table 7). Moreover, tyrosine was positively correlated to fat accumulation, while an inverse correlation was observed between plasma levels of histidine and the liver weight and liver mitochondrial respiration (Supplementary Table 7). Of note, under our experimental conditions, no statistical correlation was observed with insulin sensitivity. SFA-EAA consumption did not affect liver and kidney function parameters (Supplementary Table 6).

SFA-EAA diet extends healthy lifespan

Next, we investigated the effects of SFA-EAA diet on mouse life span. The median lifespan for chow diet-fed mice was 800 days; it was extended from 650 days for SFA mice and 680 days for SFA-CAA mice to 797 days for SFA-EAA mice (+ 23 % *versus* SFA and +17 % *versus* SFA-CAA) (Fig. 1*J*). Maximal lifespan was 899 days for chow, 800 days for SFA, 806 days for SFA-CAA, and 863 days for SFA-EAA mice. While mice fed with the SFA and SFA-CAA diet exhibited submissive/lethargic behavior after 20 months, mice fed with the SFA-EAA diet preserved energetic behavior; this was demonstrated by a test for social dominance, with a positive trend toward less fearful behavior, measured in the elevated plus-maze, and in spontaneous motor activity (Supplementary Fig. 5*A*-*C*). There was no apparent difference in novel object recognition memory test among dietary groups (Supplementary Fig. 5 *D*).

Effects on food intake and energy absorption

We then assessed energy input and output. As our mice drank only water and thus did not consume any calories through drinking, energy input was measured as food intake and energy absorption. During the first 2 or 5 days of the dietary challenge, mice fed with the EAA-substituted diets decreased their food intake compared to the respective controls; nevertheless, these differences vanished at later time points (Fig. 2*A* and Supplementary Fig. 6*A*-*C*). Similarly, the SFA-CAA- and HFD-CAA-fed mice decreased their food intake during the first days (Fig. 2*A* and Supplementary Fig. 6*A*). As these mice gained a comparable amount of body weight as SFA- and HFD-fed mice (Fig. 1*B* and Supplementary Fig. 3*A*), SFA-CAA- and HFD-CAA-fed mice served as pair-fed control to SFA-EAA- or HFD-EAA-fed mice, respectively; henceforward, the SFA-CAA and HFD-CAA diets were considered the proper control diets.

Given changes in the ratio of EAAs and nonessential amino acids (NEAAs) in both SFA-EAA and HFD-EAA *versus* casein- or CAA-containing diets, we investigated whether some of the results obtained with the SFA-EAA and HFD-EAA diets are mediated by the detection of a perturbed amino acid balance by liver or brain. We studied the activity of the critical regulator of cellular responses under amino acid deficiency sensor, the kinase general control nonderepressible 2 kinase (GCN2). When activated by accumulation of uncharged tRNAs, GCN2 phosphorylates the α subunit of eukaryotic translation initiation factor 2 (eIF2), inhibiting general protein synthesis and mitigating the cellular stress (43). We found that the SFA-EAA diet did not change the Ser51-phosphorylation of eIF2α in both hypothalamus and liver when compared to SFA and SFA-CAA diets (Supplementary Fig. 6*D*), suggesting that the effects of EAA-substituted diets are unlikely caused by detection of a dietary amino acid unbalance.

Next, we assessed the gut size and absorptive capacity of the different dietary regimens. Both SFA-EAA- and SFA-CAA-fed mice had increased transit time and jejunum villi length compared to SFA-fed animals (Fig. 2*B* and *C*); their percentage of food mass excretion was lower compared to SFA-fed mice, with only a trend to decreased amount of feces excretion (Fig. 2*D*), suggesting that both substituted diets may cause malabsorption, albeit they affect differently body weight. Thus, we investigated whether the SFA-EAA and SFA-CAA exposure led to changes in calorie uptake, by measuring the fecal caloric content with bomb calorimetry. This analysis revealed a comparable energy content in the fecal material of mice fed with SFA-EAA or SFA-CAA diet (Fig. 2*E*), resulting in similar daily energy excretion in both groups, as compared with SFA-fed mice (Fig. 2*F*), also when expressed as a percentage of the food intake. These data indicate that food malabsorption is unlikely to be the underlying cause of the SFA-EAA diet's anti-obesity action.

Effects on energy expenditure and physical activity

Next, we sought to understand whether energy expenditure was responsible for the observed phenotypes in mice fed with the different diets. The metabolic efficiency decreased in the SFA-EAA- and HFD-EAA-fed mice compared to SFA-CAA- and HFD-CAA-fed animals, respectively, starting at day 5 of treatment (Fig. 3*A* and Supplementary Fig. 7*A*), suggesting that the EAA-designer diets may target energy homeostasis to reverse the obesity-disturbed metabolism favourably. Oxygen consumption (VO_2) and energy expenditure (EE) were measured in the different dietary groups (Supplementary Table 8). Of note, while no difference was observed in mice treated for two weeks, VO_2 and EE were higher in mice fed with the EAA-substituted diets for six weeks (Fig. 3*B*, Supplementary Fig. 7*B,* and Supplementary Table 8). Locomotor activity, which is a contributor to total energy expenditure, was normal in mice fed with all of the substituted diets (Supplementary Table 8). The respiratory exchange ratio (RER) was reduced in SFA-EAA- and HFD-EAA-fed mice compared to SFA-CAA- and HFD-CAA-fed mice at both time treatment (Fig. 3*C* and Supplementary Fig. 7*C*). This result is consistent with preferential oxidation of lipid fuels in SFA-EAA and HFD-EAA mice. Moreover, the increase of core body temperature was evident only after six weeks of SFA-EAA feeding (Fig. 3*D*) and was independent of circulating levels of thyroid hormones, thyroxine (total T4) and thyroid-stimulating hormone (Supplementary Table 6). Similar results were also observed in HFD-EAA compared to HFD-CAA mice (data not shown).

Effects on gut microbiota

No significant difference in microbial richness between diets was evident with three different α-diversity estimators (Fig. 4*A*). The unsupervised multivariate statistical analysis—based on Bray-Curtis dissimilarity distance (PCoA)—showed that the gut microbiota of SFA-EAA group

represented a structural shift mainly along with the second principal component (PC2) (Fig. 4*B*). In contrast, the gut microbiota of SFA and SFA-CAA groups were not separated (Fig. 4*B*). Moreover, the Bray-Curtis dissimilarity index between SFA and SFA-EAA groups was significantly higher compared to each within-group dissimilarity and compared to that between SFA and SFA-CAA groups (FDR $P < 0.001$, Fig. 4*C*). Despite taxon-based analysis revealed small effects, the SFA-EAA diet consumption promoted an enrichment of *Allobaculum* and *Sutterella* relative abundance compared to SFA (FDR $P = 0.029$) and SFA-CAA (FDR $P = 0.032$) diet; in turn, the SFA diet enriched *Lactococcus* compared to SFA-CAA diet (FDR $P = 0.029$) (Fig. 4*D* and *E* and Supplementary Table 9). Furthermore, *Allobaculum*, *Sutterella*, and *Lactococcus* were shown as the most discriminant bacterial taxa between SFA- and SFA-EAA-fed mice by Random Forest analysis (Fig. 4*F*). Notably, *Allobaculum* relative abundance inversely correlated with the body weight (Spearman's r = –0.381, $P < 0.05$), insulin tolerance (Spearman's r= –0.529, $P < 0.005$), and glucose metabolism (Spearman's r = –0.704, $P < 0.01$). Similarly, *Sutterella* inversely correlated with the insulin tolerance (Spearman's r = –0.671, $P < 0.01$) and glucose metabolism (Spearman's r = –0.532, $P < 0.05$), as well as *Akkermansia* with a reduced body weight (Spearman's r = –0.613, $P < 0.05$).

Effects on thermogenic white adipocytes

To assess the role of adaptive thermogenesis in the action of SFA-EAA diet, we investigated whether the EAA-substituted diets were able to promote the differentiation of beige adipocytes within inguinal white adipose tissue (iWAT). Gene expression profiling after treatment did not find a statistical increase of markers of beige adipocytes in iWAT, as well as of the thermogenic genes *UCP1* and *PR domain containing 16* (*PRDM16*), the positive inducer of mitochondrial biogenesis *endothelial nitric oxide synthase* (*eNOS*) (39), or the mitochondrial biogenesis markers

in mice fed with SFA-EAA diet (Supplementary Fig. 8*A*-*C*). Moreover, the expression of genes involved in lipolysis and fatty acid oxidation remained unchanged, while NEFA levels were decreased in iWAT of SFA-EAA mice compared to controls (Supplementary Fig. 8*D*). The histological analysis confirmed these results, suggesting that browning is unlikely to play an important role in the metabolic actions of SFA-EAA diet (Supplementary Fig. 8*E*).

By contrast, we found that the uncoupled respiration was higher in iWAT mitochondria of wild-type or *ob*/*ob* mice fed with the SFA-EAA than SFA-CAA diet at 30 °C—a condition in which there is no expression of UCP1. This result suggested that the SFA-EAA diet could promote specific UCP1-independent thermogenic processes by which body temperature is increased (Fig. 5*A* and *B* and Supplementary Fig. 9*A*). Although not directly investigated at a biochemical level, gene expression analysis suggested that futile cycling, including glycerol phosphate shuttle, calcium release and reuptake, and creatine-driven substrate cycling (44) remained unchanged after consuming the SFA-EAA diet (Supplementary Fig. 10*A*-*C*), as well as mitochondrial biogenesis and function in skeletal muscle (Supplementary Fig. 10*D*-*F*). Because *N*-acyl amino acids stimulate uncoupled mitochondrial respiration in white adipocytes, independently of UCP1 (34), we also measured the levels of *N*-lipidated amino acids in both the plasma and iWAT of SFA-CAA- and SFA-EAA-fed mice, housed at 30 °C. The circulating and adipose levels of specific C18:1-amino acids were higher in SFA-EAA than SFA-CAA mice (Fig. 5*C*). The *N*-acyl amino acids were undetectable in the interscapular adipose tissue (iBAT) of mice fed with both diets. The mRNA levels of *Pm20d1* (peptidase M20 domain-containing 1), the enzyme secreted by thermogenic adipose cells that regulates *N*-acyl amino acids were unaltered in iWAT, iBAT, and liver of SFA-CAA- and SFA-EAA-fed mice (Fig. 5*D*).

Effects on brown adipocytes

Next, by using infrared thermography, we found that after 6 weeks of dietary treatment, iBAT temperature was higher in mice fed with the SFA-EAA diet compared to those fed with the SFA-CAA diet (Fig. 6*A*). Interestingly, already at day 5 of treatment, the SFA-EAA diet promoted an uncoupled respiration and the UCP1 protein expression in iBAT mitochondria compared to the control diet (Fig. 6*B* and *C*). These effects were also maintained after six weeks of treatment (Fig. 6*D* and *E*). Although thermogenic genes *type 2 iodothyronine deiodinase* (*Dio2*) and *PRDM16* were unaffected, we found an increased expression of nuclear-encoded respiratory complex genes and of mitochondrial DNA amount, in addition to *UCP1* and *eNOS*, in iBAT of mice fed with the SFA-EAA diet (Supplementary Fig. 11*A*-*C*). Moreover, the expression level of the lipolysis-related gene *adipose triglyceride lipase* (*Atgl*) was higher in iBAT of mice fed with the SFA-EAA diet than with the SFA-CAA diet (Supplementary Fig. 11*D*). This was accompanied by a greater preponderance of small lipid droplets (Supplementary Fig. 11*E*) and a higher level of NEFAs in iBAT of SFA-EAA mice (Supplementary Fig. 11*F*). These results suggested that fatty acid oxidation was increased in iBAT; accordingly, RER was decreased (Fig. 3*C*) while carnitine palmitoyltransferase 1 (CPT1) activity was increased in iBAT of mice consuming the SFA-EAA diet (Supplementary Fig. 11*G*).

The mitochondrial respiratory electron transport chain cytochrome c oxidase subunit IV (COX IV) and cytochrome c (Cyt c) protein levels were higher in iBAT of SFA-EAA than SFA-CAA mice (Fig. 6*E*), suggesting increased mitochondrial biogenesis. In accordance, the density of the mitochondrial cristae was augmented (SFA-EAA diet: 23.64 ± 0.48 μm^{-2} *versus* SFA-CAA diet: 17.83 ± 0.43 μm^{-2}; n = 600 mitochondria for each sample, $P < 0.0001$), although mitochondrial density was similar in both diets (SFA-EAA: 8.9 over 10 μm^2 *versus* SFA-CAA:

8.1 over 10 μm^2, ns) and mitochondrial area was reduced (SFA-EAA diet: 0.58 ± 0.017 μm^2 *versus* SFA diet-CAA: 0.71 ± 0.018 μm^2, $P < 0.0001$) by the SFA-EAA diet (Fig. 6*F*). Congruently, iBAT was activated in obese *ob*/*ob* mice (Supplementary Fig. 9*B*-*D*). Overall, our findings suggest that the SFA-EAA diet was able to activate an iBAT thermogenic program, in which utilization (*i.e.*, oxidation) of fatty acids is increased.

Effects on brown adipocyte activators

Thus, we investigated how the SFA-EAA diet activates thermogenic program in iBAT. Fibroblast growth factor 21 (FGF21) that promotes sympathetic nerve activity in brown fat, browning of iWAT, and energy expenditure in diet-induced obese mice (45), was lower in plasma of the SFA-EAA-fed mice, accordingly to reduced *FGF21* gene expression in liver and adipose. These observations may be of interest, since elevated circulating FGF21 is noted in impaired glucose tolerance and type 2 diabetes and correlates with muscle and hepatic insulin resistance (46), and not only with increased thermogenesis and metabolic homeostasis improvement (38). (Supplementary Fig. 12*A* and *B*). Analogously, long-chain acylcarnitines, synthesized in the liver in response to cold exposure or treatment with β_3-adrenergic receptor agonists, and providing fuel for iBAT thermogenesis (47), were unchanged in plasma of mice fed with either diet, similarly to the expression of genes involved in their metabolism in the liver, iBAT (except for *CrAT*), and muscle (Supplementary Fig. 12*C* and *D*).

Also, there was no apparent difference of norepinephrine turnover—a direct neurochemical measure of sympathetic nervous system (SNS) activity and a proxy of sympathetic innervation (48)—in iBAT of SFA-EAA mice *versus* SFA-CAA mice, as well as of tyrosine hydroxylase and β_3-adrenoceptor expression, markers of noradrenergic innervation (Fig. 7*A* and *B*). Given that

sympathetic denervation of iBAT—both surgical and chemical—has limitations, especially when used to study the involvement of SNS in systemic effects of chronic treatments, we chose to develop an *in vitro* system to confirm that the SFA-EAA diet may act directly on brown adipocytes independently of SNS. In particular, we exposed primary brown adipocytes differentiated in culture to one of two different amino acid combinations, precisely reproducing the iBAT aminograms resulting from consumption of either SFA-CAA or SFA-EAA diets (Fig. 7*C* and Supplementary Table 4). Notably, the EAA mixture increased both UCP1 mRNA and protein levels and, accordingly, the uncoupled respiration when compared to vehicle-treated cells (Fig. 7*D-F*). Conversely, the CAA mixture failed to promote either UCP1 expression or oxygen consumption. Together, these findings seem to suggest that the effects of SFA-EAA diet on iBAT depends mainly on a brown adipocyte autonomous process.

Effects on thermogenic signaling

We next aimed to investigate the molecular mechanism of iBAT activation by studying the role of the mechanistic target of rapamycin (mTOR) signaling pathway activated by amino acids and required for brown fat recruitment and metabolic adaptation to cold exposure (29,30). The exposure of primary brown adipocytes in culture to EAA mixture markedly promoted mTOR activation—as shown by the phosphorylation of the mTOR complex 1 (mTORC1)-downstream target ribosomal protein S6 (S6) (Fig. 7*G*). Despite a partial efficacy of CAA mixture in the mTOR activation, however, this effect was not associated with stimulation of the UCP1-dependent thermogenic program. In turn, rapamycin—the macrolide antibiotic that selectively inhibits mTORC1, fully antagonized the stimulatory effect of EAA mixture on the expression of UCP1 and markers of mitochondrial biogenesis (Fig. 7*E*). These results were confirmed *in vivo*, in C57BL6/N and *ob*/*ob* mice (Fig. 8 and Supplementary Fig. 13). Already at day 1 of treatment,

SFA-EAA diet consistently increased S6 phosphorylation in iBAT (Fig. 8*A*). Our data showed that this effect was iBAT-specific, without any phosphorylation of S6 and 4E-BP1 (or eukaryotic translation initiation factor 4E-binding protein 1) in iWAT and gastrocnemius muscle after 6-weeks feeding with the SFA-EAA diet (Supplementary Fig. 13*B*). The systemic administration of rapamycin entirely blocked oxygen consumption, and S6 and 4E-BP1 phosphorylation in iBAT of SFA-EAA-fed mice (Fig. 8*B* and *C*); these effects were accompanied by a blockade of action of this diet on core and iBAT temperature, UCP1 expression in brown fat, as well as on body weight and adiposity, without affecting food intake (Fig. 8*D* and *E* and Supplementary Fig. 13*C* and *D*).

DISCUSSION

Collectively, our data reveal that customized diets, in which a precise formula of EAAs substitutes for protein content—without changing calorie content and macronutrient percentage—exert preventive and therapeutic anti-obesity effects, with amelioration of body adiposity, insulin resistance, and fatty liver, beyond promoting a longer and healthier life span. The beneficial effects of either SFA-EAA or HFD-EAA diet on longevity and metabolic homeostasis can be secondary to reduced adiposity, even if the ability of our particular amino-acid combination to play a primary action cannot be excluded.

Although with the EAA-substituted diets certain EAAs (*i.e.*, histidine, isoleucine, leucine, lysine, threonine, and valine) were consumed in a higher amount, while others (*i.e.*, methionine, phenylalanine, and tyrosine) in lower amounts that those recommended for mice by the U.S. National Research Council (Supplementary Table 10), the circulating levels of EAAs and NEAAs do not seem to exceed tolerable upper and lower levels for individual amino acids. Though few studies report on the side effects of chronic intake of specific amino acid supplements, and there is no adequate dose–response data from human or animal studies to base accepted limits, our results with life-long consumption of markedly changed amino acid combination are conversely reassuring. They show that diets with very restricted—yet not wholly lacking—amounts of NEAAs (*i.e.*, the SFA-EAA and HFD-EAA diets) are healthy and do not alter animal growth. Traditionally viewed as amino acids that can be synthesized *de novo* in adequate amounts by the animal organism to meet the requirements for growth and maintenance, the nutritionally NEAAs are currently considered, in a correct way, necessary for multiple roles in physiology. NEAAs participate in gene expression, cell signalling pathways, antioxidative responses, in addition to regulate neurotransmission and immunity; thus, their non-essentiality has been questioned (42).

Reduction of food intake and gut energy absorption do not appear to play relevant roles in the healthy effects of our substituted diets. This conclusion seems to be confirmed by the absence in mice fed with SFA-EAA or HFD-EAA diets of the physiological adjustments which animals usually exhibit to maintain energy balance when subjected to a decrease in resource availability (*e.g.*, increased exploratory activities and intestinal energy absorption (49), or reduced basal metabolic rate and NST). The NST is indeed increased in SFA-EAA- and HFD-EAA-fed mice. While browning of iWAT is not induced, a UCP1's independent uncoupling of respiration is evident in iWAT of SFA-EAA-fed mice and potentially may promote thermogenesis. Despite the possibility that the observed increase of lipidated amino-acid levels in iWAT could be responsible for this higher uncoupled respiration, their relative contribution to the overall phenotype of SFA-EAA (and also of HFD-EAA) mice remains to be addressed. Most significantly, the SFA-EAA and HFD-EAA diets promote a marked iBAT activation in both normal weight and obese mice, irrespective of the environmental temperature. FGF21, acylcarnitines, NE, and thyroid hormones, well-known activators of brown fat (38,40), are not responsible for the beneficial effects of the SFA-EAA diet. Similarly, other thermogenic mechanisms, including the UCP1-independent futile cycling and muscle mitochondrial biogenesis, are not promoted by the SFA-EAA diet.

Conversely, iBAT thermogenesis could be directly activated by the specific combination of amino acids in this tissue. The EAA mixture, unlike CAA mixture—that were designed on the profiles of amino acids identified in iBAT of SFA-EAA- and SFA-CAA-fed mice (iBAT aminograms), respectively—promotes a thermogenic program in cultured brown adipocytes, through activation of mTORC1 signaling. Notably, the iBAT aminograms differ between mice fed with the two dietary regimens: arginine, isoleucine, leucine, proline, threonine, and valine are statistically higher in SFA-EAA- then in SFA-CAA-fed mice while, on the contrary, glycine, lysine, and serine are lower. From the literature, isoleucine, leucine, and valine (namely, the

branched-chain amino acids) supplementation ameliorates some metabolic dysfunction caused by obesity or diabetes, without impairing glucose metabolism, in some studies (50), but not in others (51,52). Arginine, as a substrate of nitric oxide synthase, produces nitric oxide (NO) for signaling purposes—including mitochondrial biogenesis and thermogenic program in iBAT (39). Increasing evidence has shown that dietary supplementation of arginine can effectively improve BAT thermogenesis via the mTOR signaling pathway (53), with reduced obesity and diabetes, in addition to improved obesity-linked dyslipidemia and blood hypertension in mammals, including humans (54). Similarly, proline supplementation improves NO bioavailability and counteracts the blood pressure (55). By contrast, the SFA-EAA diet reduced the NEAA glycine levels in iBAT compared to SFA-CAA diet, and accordingly, the glycine precursor threonine was increased. Of note, neuronal glycine has been found to inhibit sympathetic activation of BAT (56), and although circulating glycine is low in obese subjects, and its supplementation was proposed as a treatment of obesity (57), no clear role has been found in brown fat. Also for serine, which was similarly reduced in SFA-EAA mice, further studies are needed to confirm and extend our findings.

Additionally, we observed some interesting differences in microbiota composition. There was an enrichment of *Allobaculum* and *Sutterella* in the gut of mice fed with SFA-EAA diet compared to SFA and SFA-CAA diet, which might play some role in light of the inverse correlation we observed with body weight and insulin resistance, in agreement with previous observations (58). Several studies have demonstrated that the HFD reduces the relative abundance of both taxa in the gut of mice, while multiple dietary interventions, such as prebiotics, probiotics, and berberine—that ameliorate insulin resistance and adipose inflammation—promote the relative abundance of both *Allobaculum* and *Sutterella* (59,60). Again, mounting evidence suggests that gut microbiota can stimulate brown fat thermogenesis in mice (29,54,55). Further studies,

therefore, are warranted to establish metabolic links between gut bacteria such as *Allobaculum* and *Sutterella* and the iBAT activation by our diets.

Similarly, additional work is necessary to understand whether the pro-longevity effects of SFA-EAA are simply due to the reduced adiposity or to a direct action of our peculiar amino-acid combination. Remarkably, reducing NEAA concentration has been found to promote replicative lifespan extension in yeast (61); as in turn increasing EAA concentration prolongs the lifespan, not only in yeast, but also in *Caenorhabditis elegans* and, most importantly, in mammals (14,62,63). The increased chronological life span extension of yeast promoted by EAA supplementation was found to be accompanied by lower oxidative damage and notably by the activation, not inhibition as often reported with other life span prolonging methods, of TOR signaling pathway (61). Yang et al. (19) have moreover reported that an amino acid formula similar to the amino acid combination in our EAA-substituted diets, slowed the age-related changes of gut microbiota, without affecting body weight, suggesting that the dietary supplementation might promote healthy aging independently of its effects on adiposity.

Since our EAA-substituted diets are deficient of some EAA compared to controls, one could claim that detection of amino acid unbalance or, alternately, a restriction of specific amino acids may be relevant intermediaries to the beneficial effects of both SFA-EAA and HFD-EAA diets. These possibilities were proposed to interpret previous findings. For example, mice fed with diets lacking the single EAA tryptophan had increased resistance to surgical stress, as well as improved longevity, metabolic fitness and stress resistance (64). However, detection of dietary amino acid imbalance seems improbable in our case since there is no apparent change of the GCN2 activity, the critical regulator of cellular responses under amino acid deficiency or imbalance, in both hypothalamus and liver of mice under the different dietary regimens. Moreover, previous studies have shown that diets deficient in EAAs can influence food intake and increase FGF21

levels (65). Consuming SFA-EAA diet, conversely, does not change feeding and decreases circulating and hepatic FGF21 levels. Also, feeding rodents survival-promoting methionine-restricted diets comprising purified amino acids as the sole source of nitrogenous content causes some of the phenotypes described here, including protection from weight gain (mostly in adiposity), improved glucose homeostasis, increased energy expenditure, and activation of iBAT (66). However, the abundance of cysteine in SFA-EAA and HFD-EAA diets rules out methionine-restriction as the key mechanism behind the present findings.

In summary, the present study indicates that specific manipulation of dietary amino acids prevents and reverses obesity in mice through multiple modes to stimulate thermogenesis. Reasonably, taken separately each other, these multiple modes would be unable to explain the overall observed results. If extended to humans, such dietary manipulation could potentially have a positive impact on metabolic health favoring the prevention and treatment of obesity and type 2 diabetes regardless of calorie consumption.

Acknowledgments. The authors thank M. Rossato (Department of Medicine, University of Padua, Padua, Italy) for experiments with the Flir camera; Mariaelvina Sala and Daniela Braida (Department of Medical Biotechnology and Translational Medicine, University of Milan, Milan, Italy) for behavioral experiments; Annapaola Andolfo and Cinzia Magagnotti (Protein Microsequencing Facility, San Raffaele Scientific Institute, Milan, Italy) for mass spectrometry analysis, and Alessandra Micheletti (Department of Environmental Sciences and Politics, University of Milan, Milan, Italy) and Marika Vezzoli (Department of Molecular and Translational Medicine, Brescia University, Brescia, Italy) for statistical analysis.

Funding. This work was supported by Fondazione Umberto Veronesi to C.R., University of Milan to F.R. (Research Fellowship grant 1280/2016), Professional Dietetics (Milan, Italy) to E.N. (support to laboratory), Cariplo Foundation to E.N. and to A.V. (grant 2016-1006), and Louis-Jeantet Foundation grant to R.C.

Duality of Interests. No potential conflicts of interest relevant to this article were reported.

Author Contributions. C.R. and M.R. designed and performed molecular biology, metabolic, oxygen consumption, and animal experiments; P.C., C.G., D.L., and R.P.C. designed and performed experiments in animals; V.G., L.Tenori, and C.L. designed and analyzed experiments on metabolites; R.M.I., F.Bontems, and R.C. designed, performed, and analyzed indirect calorimetry experiments; A.C., F.P. and V.D. designed, performed, and analyzed liquid chromatography-mass spectroscopy experiments for *N*-acyl-amino acid and acylcarnitine measurements; E.M. synthesized *N*-acyl-amino acids; L.Tedesco and F.R. performed *in vitro* experiments and qRT-PCR analysis; A.P. and I.D. performed experiments at thermoneutrality;

L.P. designed, performed, and analyzed behavioral experiments; L.R., M.U.S., and K.T. performed microbiota analysis; I.S. and S.Cinti designed, performed, and analyzed electron microscopy and histological experiments; F.B., M.O.C, G.C., R.C., S.Collins, and A.V. assisted with experimental design and co-edited the manuscript; E.N. conceived the study, designed experiments, and provided advice; C.R., M.R., and E.N. wrote the manuscript with suggestions from all authors, all of whom read and approved the final version. E.N. is the guarantor of this work and, as such, had full access to all the data in the study and takes responsibility for the integrity of the data and the accuracy of the data analysis.

Figure Legends

Figure 1 — EAA, unlike CAA substitution for protein content of rodent diets prevents and reverses obesity, with the improvement of glucose homeostasis and extension of average lifespan. *A*: Body weight of mice fed with chow, SFA, SFA-EAA, and SFA-CAA diet at room temperature (n = 7-10 mice per group). After maximal body weight was reached (11 months, dashed line), mice fed with SFA were switched to either SFA-EAA diet (SFA > SFA-EAA) or SFA-CAA diet (SFA > SFA-CAA) (n = 5 mice per group). *B*: Body weight of mice at room temperature (n = 9-10 mice per group). *C*: Body composition at the end of treatment: fat mass (left) and lean mass (right) (n = 6 mice per group). *D*: Plasma leptin levels at different time points at room temperature (n = 5 mice per group). *E*: Body weight of mice at thermoneutrality (30 °C) (n = 10 mice per group). *F* and *G*: Glucose tolerance tests (GTT) in mice at room temperature (n = 5 mice per group) (*F*) or at thermoneutrality (*G*) (n = 7 mice per group). Mice were fed with different diets for six weeks. *H* and *I*: Plasma levels of adiponectin (*H*) and IGF-1 (*I*) in mice fed with SFA-CAA and SFA-EAA diet for six weeks at room temperature (n = 5 mice per group). *J*: Kaplan-Meier survival curves for chow, SFA, SFA-EAA, and SFA-CAA-fed mice (n = 35 mice per group). All data (except *J*) are presented as mean ± SEM. $^{*}P < 0.05$, $^{**}P < 0.01$, and $^{***}P < 0.001$ vs. SFA diet, $^{\#}P < 0.05$, $^{\#\#}P < 0.01$, and $^{\#\#\#}P < 0.001$ vs. SFA-CAA diet, $^{\S}P < 0.05$, $^{\S\S}P < 0.01$, and $^{\S\S\S}P < 0.001$ vs. chow diet.

Figure 2 — Food intake and energy absorption in mice on different dietary regimens. *A*: Food intake of mice fed with chow, SFA, SFA-EAA, and SFA-CAA diets for different time intervals (n = 5-7 mice per group). *B*: Gut transit time. *C*: hematoxylin and eosin staining of jejunum villi. Scale bar, 90 μm. *D*: energy excretion: the mean amount of feces excreted per mouse in 24 h

(mg/24 h) (*left*) and food excreted (dry mass of fecal pellets, collected over 72 h and expressed as the percentage of food intake) (*right*). *E*: mean energy content in feces (kcal/g). *F*: daily energy excretion (kcal/mouse) calculated using the previous values (n = 3–5 mice per group). *B*-*F*: mice were fed with SFA, SFA-CAA, and SFA-EAA diets for six weeks. All data are presented as mean ± SEM. $^{**}P < 0.01$ and $^{***}P < 0.001$ vs. SFA diet; $^{\#\#\#}P < 0.001$ vs. SFA-CAA; $^{\S\S\S}P < 0.001$ vs. chow diet.

Figure 3 — Energy metabolism in mice on different dietary regimens. *A*: Metabolic efficiency was calculated as the body weight gain to the energy intake ratio (*i.e.*, total food consumed during five days or 2 or 6 weeks). *B* and *C*: Energy expenditure (*B*) and respiratory exchange ratio (RER) (*C*) during one 24 h cycle. *D*: Whole-body temperature measured with a digital rectal thermometer. Measurements were performed in two separate experiments, after 2 or 6 weeks (n = 5-7 mice per group). All data are presented as mean ± SEM. $^{*}P < 0.05$, $^{**}P < 0.01$, and $^{***}P < 0.001$ vs. SFA-CAA diet.

Figure 4 — SFA-EAA diet changes gut microbiota composition. *A*: Chao index, Shannon entropy index, and alpha-diversity calculated on the number of observed OTUs. *B*: Principal coordinates analysis (PCoA) of bacterial beta-diversity based on the Bray-Curtis dissimilarity index. Each symbol represents a single sample of feces after six weeks of treatment. *C*: Box-and-whisker plot of intercommunity beta-diversity determined by Bray-Curtis dissimilarity index. *D*: Phylum/order level relative abundance expressed as geometric mean. *E*: *Allobaculum*, *Sutterella*, and *Lactococcus* relative abundance. *F*: Random Forest analysis. For box-and-whisker plots, boxes show median, first and third quartiles. The whiskers extend from the quartiles to the last data point

within 1.5× IQR, with outliers beyond represented as dots (n = 10 mice per group). *P < 0.05, **P < 0.01, and ***P< 0.001 as shown.

Figure 5 — SFA-EAA diet promotes uncoupled respiration in inguinal WAT (iWAT) without browning stimulation. *A*: Uncoupled (*i.e.*, with oligomycin) and maximal (*i.e.*, with FCCP) oxygen consumption rates (OCR) in iWAT mitochondria; respiration was normalized to mitochondrial protein amount (n = 5 mice per group). *B*: Western blot analysis of UCP1 and HSP60 protein levels in adipose tissues (n = 4 mice per group). One experiment representative of three reproducible ones is shown. iBAT of mice fed with chow diet at room temperature was used as control. *C*: Thermogenic *N*-acyl amino acids in plasma (*left*) and iWAT (*right*) (n = 4-5 mice per group). *D*: Relative mRNA levels of *Pm20d1* gene in different tissues (n = 5 mice per group). *A-D*, mice were fed with SFA-CAA and SFA-EAA diet for six weeks at thermoneutrality. All data are presented as mean ± SEM. *P < 0.05, **P < 0.01, and ***P < 0.001 vs. SFA-CAA diet.

Figure 6 — SFA-EAA diet increases the thermogenic function of iBAT. *A*: iBAT temperature was measured with thermographic Flir camera in mice fed with SFA-CAA and SFA-EAA diet for six weeks at room temperature (n = 5 mice per group). *B*: Uncoupled (*i.e.,* ΔGDP, UCP1-dependent respiration calculated as the amount of ADP-independent respiration that was inhibited by GDP) and maximal (FCCP) oxygen consumption rates (OCR) in iBAT mitochondria; respiration was normalized to mitochondrial protein amount (n = 5 mice per group). *C*: Western blot analysis of UCP1 and GAPDH protein levels in iBAT. One experiment representative of three reproducible ones is shown (n = 3-5 mice per group). Mice in *B* and *C* were fed with SFA-CAA and SFA-EAA diet for 1, 5, or 20 days at room temperature. *D*: Uncoupled (ΔGDP) and maximal (FCCP) OCR in iBAT mitochondria (n = 6 mice per group). *E*: Western blot analysis of UCP1, COX IV, Cyt c,

and GAPDH protein levels in iBAT. One experiment representative of three reproducible ones (n = 4 mice per group). *F*: Electron microscopy analysis of iBAT. Scale bar, 0.5 μm (n = 2 mice per group). Mice in *D-F* were fed with SFA-CAA and SFA-EAA diet for six weeks at room temperature. All data are presented as mean ± SEM. *$P < 0.05$ and **$P < 0.01$ vs. SFA-CAA diet. UCP1, uncoupling protein 1; COX-IV, cytochrome c oxidase subunit IV; Cyt c, cytochrome c; GAPDH, glyceraldehyde 3-phosphate dehydrogenase.

Figure 7 — SFA-EAA diet activates brown adipocytes. *A*: Norepinephrine (NE) turnover (NETO) in iBAT of mice fed with SFA-CAA and SFA-EAA diet for six weeks at room temperature. NETO was assessed by NE synthesis inhibition with α-methyl-p-tyrosine (n = 5 mice per group). *B*: Relative mRNA levels of noradrenergic innervation markers in iBAT of mice fed with SFA-CAA and SFA-EAA diet for six weeks. *C*: Scheme of *in vitro* experiment in primary brown adipocytes isolated from mice fed with chow diet. After 16 h incubation in amino acid-free medium, brown adipocytes were pretreated with rapamycin (Rapa, 1.0 nM) or Veh (DMSO) for one h. Then, the cells were supplemented with Veh (PBS) or CAAm or EAAm, specifically reproducing the iBAT aminograms resulting from consumption of either SFA-CAA or SFA-EAA diets, respectively, as reported in Supplementary Table 4 (n = 3 experiments performed in triplicate). *D*: *UCP1* mRNA levels in differentiated brown adipocytes, treated as in *C*. *E* and *G*: Western blot analysis of UCP1 and GAPDH (*E*), and (Ser 235/236) phosphorylated S6 and S6 (*G*) protein levels in differentiated brown adipocytes, treated as in *C*. One immunoblot experiment representative of three reproducible ones. *F*: Oxygen consumption rates (OCR) of differentiated brown adipocytes, treated as in *C*. OCR was measured with Seahorse XF24 Extracellular Flux Analyzer (n = 3 readings in quadruplicate/group). All data are presented as mean ± SEM. **$P < 0.01$ and ***$P < 0.001$ vs. Veh; $^{\#}P < 0.05$, $^{\#\#}P < 0.01$, and $^{\#\#\#}P < 0.001$ vs. CAAm; $^{\S}P < 0.05$ and $^{\S\S\S}P < 0.001$ vs.

EAAm + Rapa. TH, tyrosine hydroxylase; β_3AR, β_3-adrenergic receptor; CAAm, casein amino-acid mixture; EAAm, essential amino-acid mixture; UCP1, uncoupling protein 1; GAPDH, glyceraldehyde 3-phosphate dehydrogenase; S6, ribosomal protein S6.

Figure 8 — mTORC1 signaling contributes to iBAT thermogenesis induced by SFA-EAA diet. *A*: Western blot analysis of (Ser 235/236) phosphorylated S6 and S6 protein levels in iBAT of mice fed with SFA-CAA and SFA-EAA diet for different time intervals at room temperature. One immunoblot experiment representative of three reproducible ones (n = 3-5 mice per group). *B*: Western blot analysis of the mTORC1 pathway in iBAT of mice fed with SFA-CAA and SFA-EAA diet, with vehicle (Veh) or rapamycin (Rapa) (n = 4 mice per group). *C*: UCP1-dependent (ΔGDP) and maximal (FCCP) oxygen consumption rates (OCR) in iBAT mitochondria. OCR was normalized to mitochondrial protein amount (n = 5 mice per group). *D*: Rectal and thermographic measurement of iBAT temperature (n = 5 mice per group). *E*: Western blot analysis of UCP1 protein levels in iBAT. Mice in *B*-*E* were fed with SFA-CAA and SFA-EAA diet for six weeks at room temperature, with or without rapamycin (i.p. 2.5 mg/kg body weight) delivered in 200 µl, 5 days per week for six weeks, starting with diets (n = 5-6 mice per group). All data are presented as mean ± SEM. *$P < 0.05$, **$P < 0.01$, and ***$P < 0.001$ vs. SFA-CAA diet; $^{\#}P < 0.05$ vs. SFA-EAA diet. S6, ribosomal protein S6; 4E-BP1, eukaryotic initiation factor 4E-binding protein 1 phosphorylation; UCP1, uncoupling protein 1.

References

1. Koska J, Ozias MK, Deer J, Kurtz J, Salbe AD, Harman SM, et al. A human model of dietary saturated fatty acid induced insulin resistance. Metabolism 2016;65:1621–8
2. Vasilopoulou D, Markey O, Kliem KE, Fagan CC, Grandison AS, Humphries DJ, et al. Reformulation initiative for partial replacement of saturated with unsaturated fats in dairy foods attenuates the increase in LDL cholesterol and improves flow-mediated dilatation compared with conventional dairy: the randomized, controlled REplacement of. Am J Clin Nutr 2020;1–10
3. Scherer PE. The many secret lives of adipocytes: implications for diabetes. Diabetologia 2019;62:223–32
4. Hall KD, Ayuketah A, Brychta R, Cai H, Cassimatis T, Chen KY, et al. Ultra-Processed Diets Cause Excess Calorie Intake and Weight Gain: An Inpatient Randomized Controlled Trial of Ad Libitum Food Intake. Cell Metab 2019;30:67–77
5. Gardner CD, Kiazand A, Alhassan S, Kim S, Stafford RS, Balise RR, et al. Comparison of the Atkins, Zone, Ornish, and LEARN diets for change in weight and related risk factors among overweight premenopausal women: The A to Z weight loss study: A randomized trial. J Am Med Assoc 2007;297:969–77
6. Lagiou P, Sandin S, Lof M, Trichopoulos D, Adami HO, Weiderpass E. Low carbohydrate-high protein diet and incidence of cardiovascular diseases in Swedish women: Prospective cohort study. BMJ 2012;345:7864
7. Huang X, Hancock DP, Gosby AK, McMahon AC, Solon SMC, Le Couteur DG, et al. Effects of dietary protein to carbohydrate balance on energy intake, fat storage, and heat production in mice. Obesity (Silver Spring) 2013;21:85–92
8. Fontana L, Cummings NE, Arriola Apelo SI, Neuman JC, Kasza I, Schmidt BA, et al. Decreased Consumption of Branched-Chain Amino Acids Improves Metabolic Health. Cell Rep 2016;16:520–30
9. Anthony TG, Morrison CD, Gettys TW. Remodeling of lipid metabolism by dietary restriction of essential amino acids. Diabetes 2013;62:2635–44
10. Binder E, Bermúdez-Silva FJ, André C, Elie M, Romero-Zerbo SY, Leste-Lasserre T, et al. Leucine supplementation protects from insulin resistance by regulating adiposity levels. PLoS One 2013;8:e74705
11. Serra F, LeFeuvre RA, Slater D, Palou A, Rothwell NJ. Thermogenic actions of tryptophan in the rat are mediated independently of 5-HT. Brain Res 1992;578:327–34
12. Nairizi A, She P, Vary TC, Lynch CJ. Leucine Supplementation of Drinking Water Does Not Alter Susceptibility to Diet-Induced Obesity in Mice. J Nutr. 2009 Apr;139(4):715–9.
13. Bifari F, Nisoli E. Branched-chain amino acids differently modulate catabolic and anabolic states in mammals: a pharmacological point of view. Br J Pharmacol. 2017;174(11).
14. D'Antona G, Ragni M, Cardile A, Tedesco L, Dossena M, Bruttini F, et al. Branched-chain amino acid supplementation promotes survival and supports cardiac and skeletal muscle mitochondrial biogenesis in middle-aged mice. Cell Metab 2010;12:362–72
15. D'Antona G, Tedesco L, Ruocco C, Corsetti G, Ragni M, Fossati A, et al. A Peculiar Formula of Essential Amino Acids Prevents Rosuvastatin Myopathy in Mice. Antioxidants Redox Signal 2016;25:11
16. Bifari F, Dolci S, Bottani E, Pino A, Di Chio M, Zorzin S, et al. Complete neural stem cell (NSC) neuronal differentiation requires a branched chain amino acids-induced persistent metabolic shift towards energy metabolism. Pharmacol Res 2020;158:104863

17. Brunetti D, Bottani E, Segala A, Marchet S, Rossi F, Malavolta M, et al. Targeting multiple mitochondrial processes by a metabolic modulator prevents sarcopenia and cognitive decline in SAMP8 mice. Front Pharmacol. 2020;11:1171
18. Buondonno I, Sassi F, Carignano G, Dutto F, Ferreri C, Pili FG, et al. From mitochondria to healthy aging: The role of branched-chain amino acids treatment: MATeR a randomized study. Clin Nutr 2020;39:2080–91
19. Yang Z, Huang S, Zou D, Dong D, He X, Liu N, et al. Metabolic shifts and structural changes in the gut microbiota upon branched-chain amino acid supplementation in middle-aged mice. Amino Acids 2016;48:2731–45
20. Ridaura VK, Faith JJ, Rey FE, Cheng J, Duncan AE, Kau AL, et al. Gut microbiota from twins discordant for obesity modulate metabolism in mice. Science 2013;341:1241214
21. Sharon G, Garg N, Debelius J, Knight R, Dorrestein PC, Mazmanian SK. Specialized metabolites from the microbiome in health and disease. Cell Metab 2014;20:719–30
22. Cox LM, Yamanishi S, Sohn J, Alekseyenko A V., Leung JM, Cho I, et al. Altering the intestinal microbiota during a critical developmental window has lasting metabolic consequences. Cell 2014;158:705–21
23. Li B, Li L, Li M, Lam SM, Wang G, Wu Y, et al. Microbiota Depletion Impairs Thermogenesis of Brown Adipose Tissue and Browning of White Adipose Tissue. Cell Rep 2019;26:2720–37
24. Shabalina IG, Petrovic N, de Jong JMA, Kalinovich AV, Cannon B, Nedergaard J. UCP1 in Brite/Beige Adipose Tissue Mitochondria Is Functionally Thermogenic. Cell Rep 2013;5:1196–203
25. Cohen P, Levy JD, Zhang Y, Frontini A, Kolodin DP, Svensson KJ, et al. Ablation of PRDM16 and beige adipose causes metabolic dysfunction and a subcutaneous to visceral fat switch. Cell 2014;156:304–16
26. Lowell BB, S-Susulic V, Hamann A, Lawitts JA, Himms-Hagen J, Boyer BB, et al. Development of obesity in transgenic mice after genetic ablation of brown adipose tissue. Nature 1993;366:740–2
27. Feldmann HM, Golozoubova V, Cannon B, Nedergaard J. UCP1 ablation induces obesity and abolishes diet-induced thermogenesis in mice exempt from thermal stress by living at thermoneutrality. Cell Metab 2009;9:203–9
28. Seale P, Conroe HM, Estall J, Kajimura S, Frontini A, Ishibashi J, et al. Prdm16 determines the thermogenic program of subcutaneous white adipose tissue in mice. J Clin Invest 2011;121:96–105
29. Liu D, Bordicchia M, Zhang C, Fang H, Wei W, Li J-L, et al. Activation of mTORC1 is essential for β-adrenergic stimulation of adipose browning. J Clin Invest 2016;126:1704–16
30. Labbé SM, Mouchiroud M, Caron A, Secco B, Freinkman E, Lamoureux G, et al. MTORC1 is Required for Brown Adipose Tissue Recruitment and Metabolic Adaptation to Cold. Sci Rep 2016;6: 37223
31. Brown LJ, Koza RA, Everett C, Reitman ML, Marshall L, Fahien LA, et al. Normal thyroid thermogenesis but reduced viability and adiposity in mice lacking the mitochondrial glycerol phosphate dehydrogenase. J Biol Chem 2002;277:32892–8
32. Ikeda K, Kang Q, Yoneshiro T, Camporez JP, Maki H, Homma M, et al. UCP1-independent signaling involving SERCA2b-mediated calcium cycling regulates beige fat thermogenesis and systemic glucose homeostasis. Nat Med 2017;23:1454–65
33. Kazak L, Chouchani ET, Lu GZ, Jedrychowski MP, Bare CJ, Mina AI, et al. Genetic

Depletion of Adipocyte Creatine Metabolism Inhibits Diet-Induced Thermogenesis and Drives Obesity. Cell Metab 2017;26: 660-671
34. Long JZ, Svensson KJ, Bateman LA, Lin H, Kamenecka T, Lokurkar IA, et al. The Secreted Enzyme PM20D1 Regulates Lipidated Amino Acid Uncouplers of Mitochondria. Cell 2016;166:424–35
35. Fontaine DA, Davis DB. Attention to background strain is essential for metabolic research: C57BL/6 and the international knockout mouse consortium. Diabetes 2016;65:25–33
36. Ramadori G, Fujikawa T, Fukuda M, Anderson J, Morgan DA, Mostoslavsky R, et al. SIRT1 deacetylase in POMC neurons is required for homeostatic defenses against diet-induced obesity. Cell Metab 2010;12:78–87
37. Chevalier C, Stojanović O, Colin DJ, Suarez-Zamorano N, Tarallo V, Veyrat-Durebex C, et al. Gut Microbiota Orchestrates Energy Homeostasis during Cold. Cell 2015;163:1360–74
38. Lister RG. The use of a plus-maze to measure anxiety in the mouse. Psychopharmacology (Berl) 1987;92:180–5
39. Nisoli E. Mitochondrial Biogenesis in Mammals: The Role of Endogenous Nitric Oxide. Science 2003;299:896–9
40. Bieber LL, Abraham T, Helmrath T. A rapid spectrophotometric assay for carnitine palmitoyltransferase. Anal Biochem 1972;50:509–18
41. Gordon CJ. The mouse thermoregulatory system: Its impact on translating biomedical data to humans. Physiol Behav 2017;179:55–66
42. Kanazawa I, Yamaguchi T, Sugimoto T. Serum insulin-like growth factor-I is negatively associated with serum adiponectin in type 2 diabetes mellitus. Growth Horm IGF Res 2011;21:268–71
43. Dever TE, Feng L, Wek RC, Cigan AM, Donahue TF, Hinnebusch AG. Phosphorylation of initiation factor 2α by protein kinase GCN2 mediates gene-specific translational control of GCN4 in yeast. Cell 1992;68:585–96
44. Chouchani ET, Kazak L, Spiegelman BM. New Advances in Adaptive Thermogenesis: UCP1 and Beyond. Cell Metab 2019;29:27–37
45. Kliewer SA, Mangelsdorf DJ. A Dozen Years of Discovery: Insights into the Physiology and Pharmacology of FGF21. Cell Metab 2019;29:246–53
46. Chavez AO, Molina-Carrion M, Abdul-Ghani MA, Folli F, Defronzo RA, Tripathy D. Circulating fibroblast growth factor-21 is elevated in impaired glucose tolerance and type 2 diabetes and correlates with muscle and hepatic insulin resistance. Diabetes Care 2009;32:1542–6
47. Simcox J, Geoghegan G, Maschek JA, Bensard CL, Pasquali M, Miao R, et al. Global Analysis of Plasma Lipids Identifies Liver-Derived Acylcarnitines as a Fuel Source for Brown Fat Thermogenesis. Cell Metab 2017;26:509-522
48. Vaughan CH, Zarebidaki E, Ehlen JC, Bartness TJ. Analysis and measurement of the sympathetic and sensory innervation of white and brown adipose tissue. Methods Enzymol 2014;537:199–225
49. Peña-Villalobos I, Casanova-Maldonado I, Lois P, Sabat P, Palma V. Adaptive Physiological and Morphological Adjustments Mediated by Intestinal Stem Cells in Response to Food Availability in Mice. Front Physiol 2018;9:1821
50. Woo S-L, Yang J, Hsu M, Yang A, Zhang L, Lee R-P, et al. Effects of branched-chain amino acids on glucose metabolism in obese, prediabetic men and women: a randomized, crossover study. Am J Clin Nutr 2019;109:1569–77

51. Newgard CB, An J, Bain JR, Muehlbauer MJ, Stevens RD, Lien LF, et al. A branched-chain amino acid-related metabolic signature that differentiates obese and lean humans and contributes to insulin resistance. Cell Metab 2009;9:311–26
52. Zhou M, Shao J, Wu CY, Shu L, Dong W, Liu Y, et al. Targeting BCAA catabolism to treat obesity-associated insulin resistance. Diabetes 2019;68:1730–46
53. Ma X, Han M, Li D, Hu S, Gilbreath KR, Bazer FW, et al. l-Arginine promotes protein synthesis and cell growth in brown adipocyte precursor cells via the mTOR signal pathway. Amino Acids 2017;49:957–64
54. McKnight JR, Satterfield MC, Jobgen WS, Smith SB, Spencer TE, Meininger CJ, et al. Beneficial effects of L-arginine on reducing obesity: Potential mechanisms and important implications for human health. Vol. 39, Amino Acids. Springer-Verlag Wien; 2010. p. 349–57.
55. Leal J, Teixeira-Santos L, Pinho D, Afonso J, Carvalho J, de Lourdes Bastos M, et al. L-proline supplementation improves nitric oxide bioavailability and counteracts the blood pressure rise induced by angiotensin II in rats. Nitric Oxide - Biol Chem 2019;82:1–11
56. Conceição EPS da, Madden CJ, Morrison SF. Glycinergic inhibition of BAT sympathetic premotor neurons in rostral raphe pallidus. Am J Physiol Regul Integr Comp Physiol 2017;312:R919–26
57. Alves A, Bassot A, Bulteau AL, Pirola L, Morio B. Glycine metabolism and its alterations in obesity and metabolic diseases. Nutrients 2019;11:1356
58. Schneeberger M, Everard A, Gómez-Valadés AG, Matamoros S, Ramírez S, Delzenne NM, et al. Akkermansia muciniphila inversely correlates with the onset of inflammation, altered adipose tissue metabolism and metabolic disorders during obesity in mice. Sci Rep 2015;5:16643
59. Everard A, Matamoros S, Geurts L, Delzenne NM, Cani PD. Saccharomyces boulardii administration changes gut microbiota and reduces hepatic steatosis, low-grade inflammation, and fat mass in obese and type 2 diabetic db/db mice. MBio 2014; 5:e01011-14
60. Zhang X, Zhao Y, Zhang M, Pang X, Xu J, Kang C, et al. Structural changes of gut microbiota during berberine-mediated prevention of obesity and insulin resistance in high-fat diet-fed rats. PLoS One 2012;7:e42529
61. Jiang JC, Jaruga E, Repnevskaya M V, Jazwinski SM. An intervention resembling caloric restriction prolongs life span and retards aging in yeast. FASEB J 2000;14:2135–7
62. Aris JP, Alvers AL, Ferraiuolo RA, Fishwick LK, Hanvivatpong A, Hu D, et al. Autophagy and leucine promote chronological longevity and respiration proficiency during calorie restriction in yeast. Exp Gerontol 2013;48:1107–19
63. Edwards C, Canfield J, Copes N, Brito A, Rehan M, Lipps D, et al. Mechanisms of amino acid-mediated lifespan extension in Caenorhabditis elegans. BMC Genet. 2015;16(1):1–24.
64. Gallinetti J, Harputlugil E, Mitchell JR. Amino acid sensing in dietary-restriction-mediated longevity: roles of signal-transducing kinases GCN2 and TOR. Biochem J 2013;449:1–10
65. De Sousa-Coelho AL, Marrero PF, Haro D. Activating transcription factor 4-dependent induction of FGF21 during amino acid deprivation. Biochem J 2012;443:165–71
66. Wanders D, Burk DH, Cortez CC, Van NT, Stone KP, Baker M, et al. UCP1 is an essential mediator of the effects of methionine restriction on energy balance but not insulin sensitivity. FASEB J 2015;29:2603–15

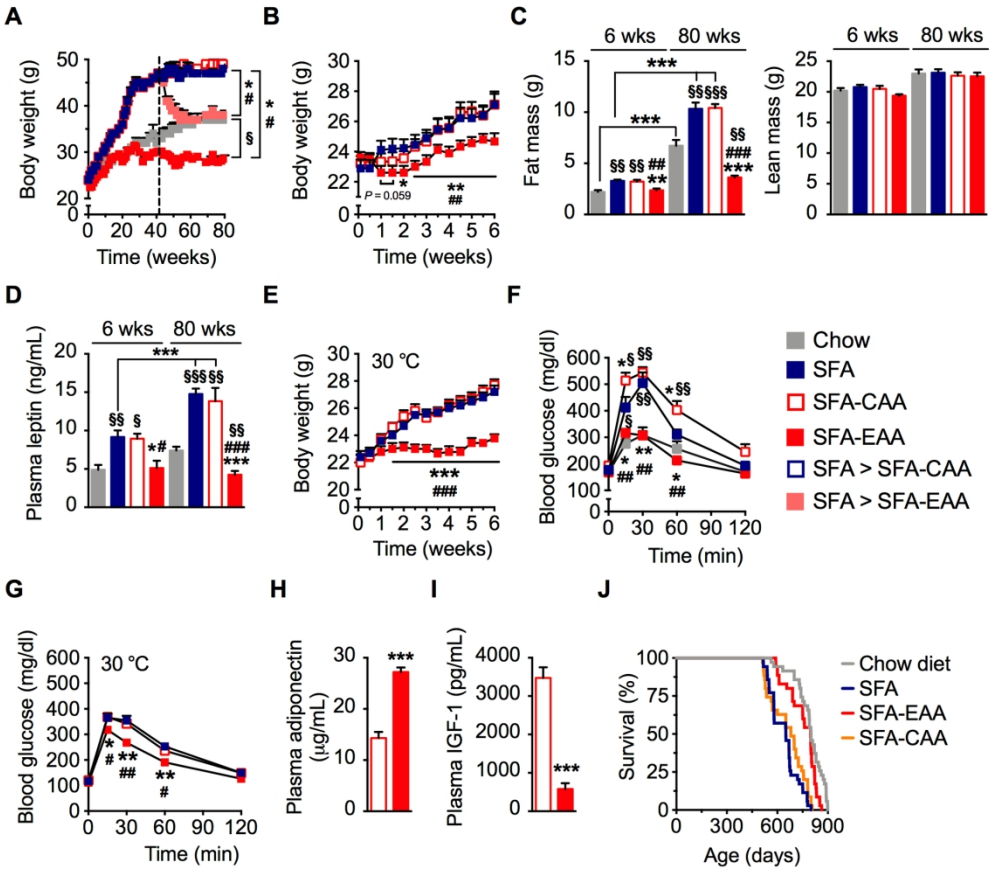

Figure 1

180x159mm (300 x 300 DPI)

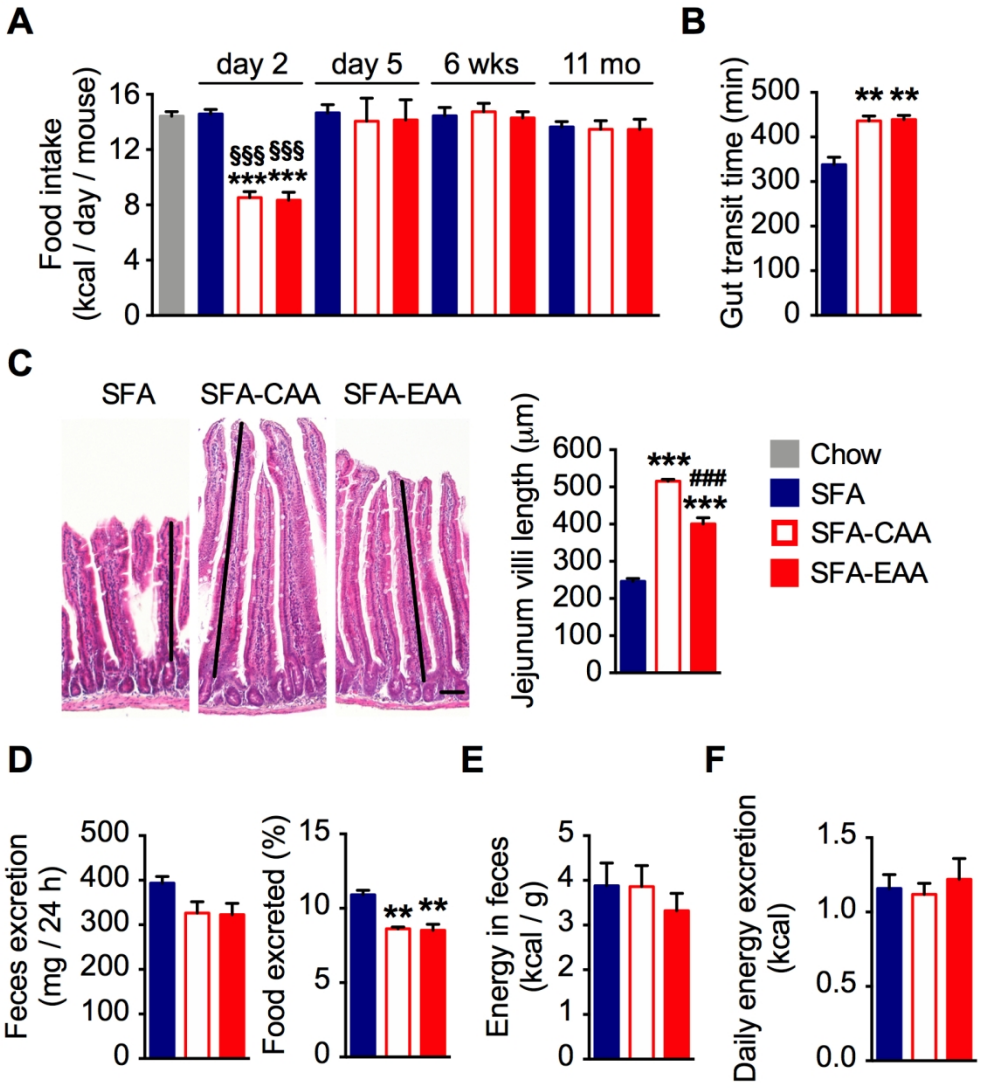

Figure 2

135x150mm (300 x 300 DPI)

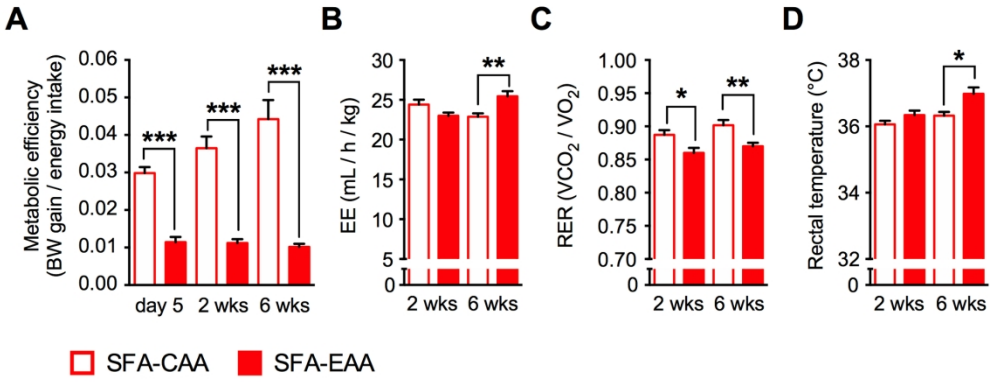

Figure 3

180x70mm (300 x 300 DPI)

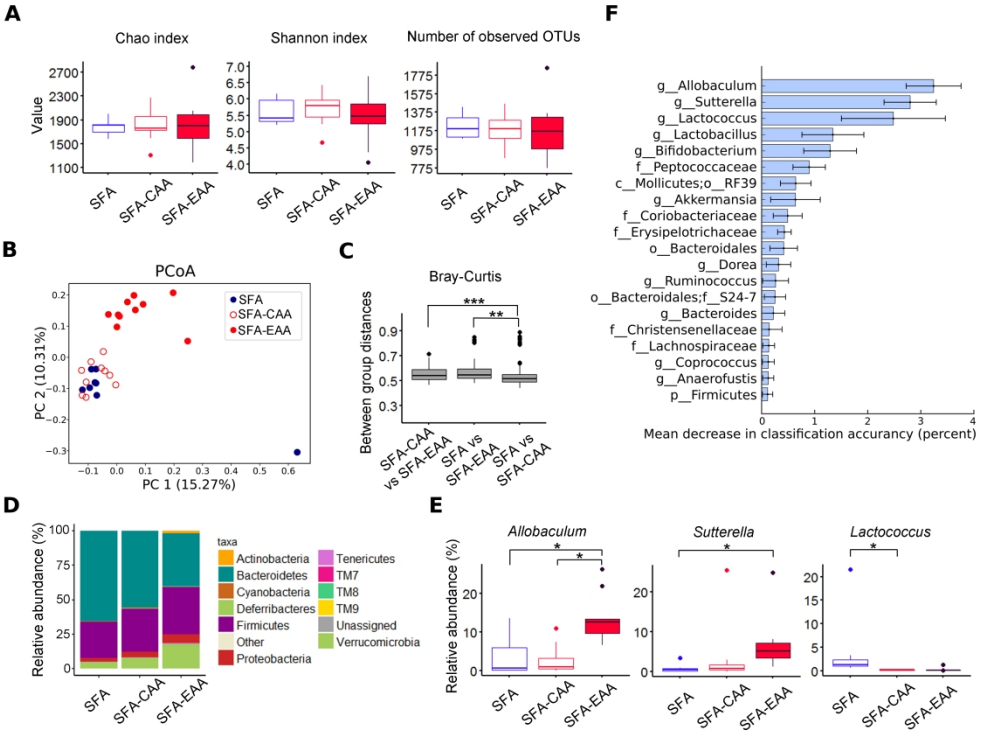

Figure 4

179x135mm (567 x 567 DPI)

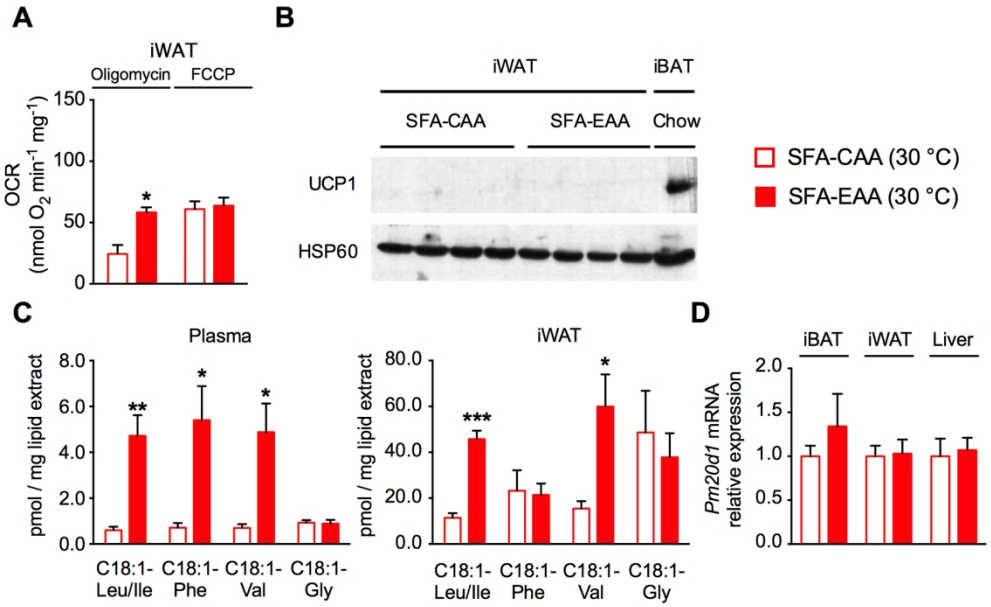

Figure 5

180x111mm (300 x 300 DPI)

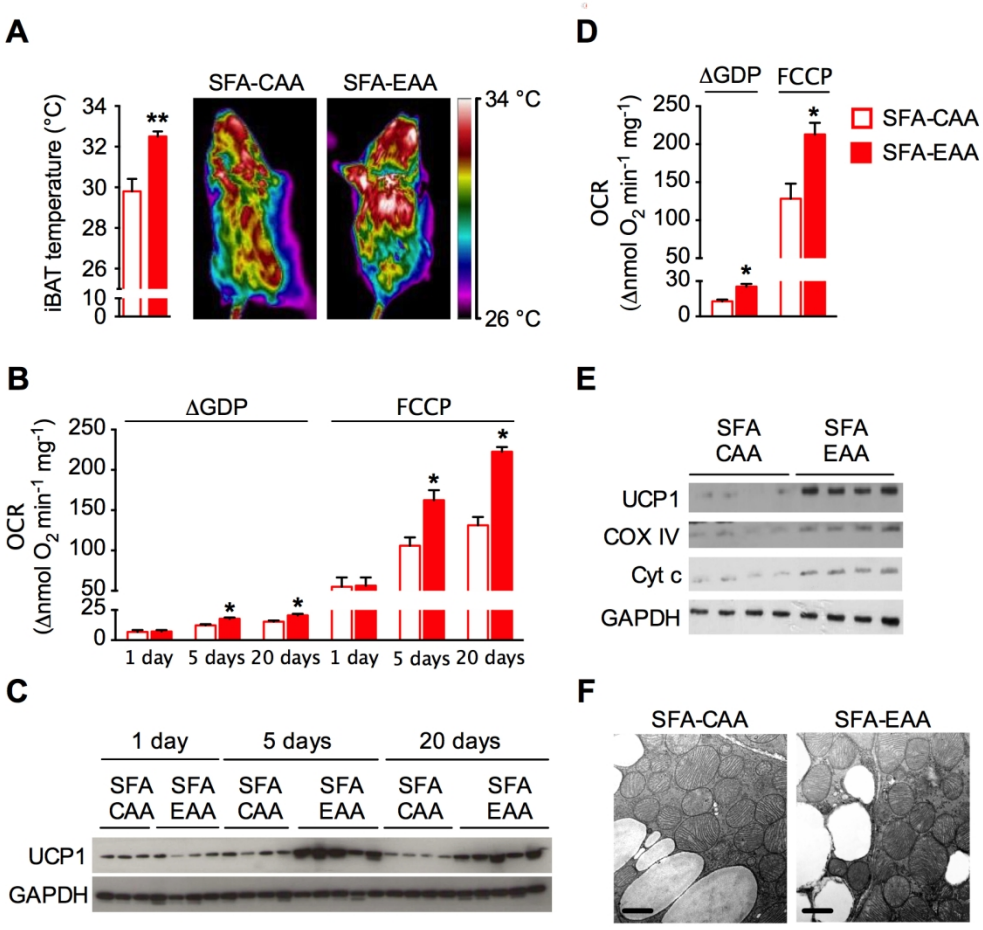

Figure 6

155x143mm (300 x 300 DPI)

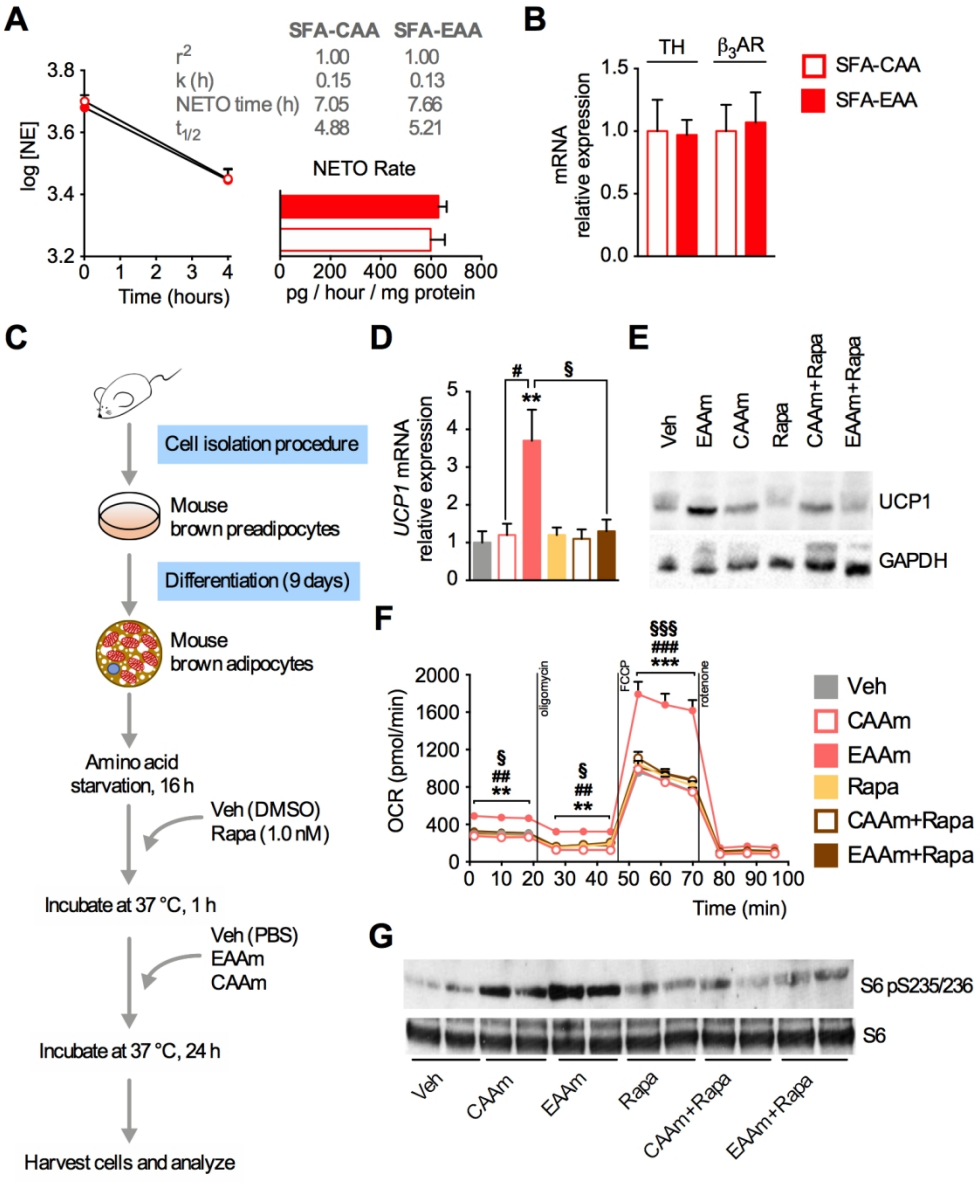

Figure 7

137x165mm (300 x 300 DPI)

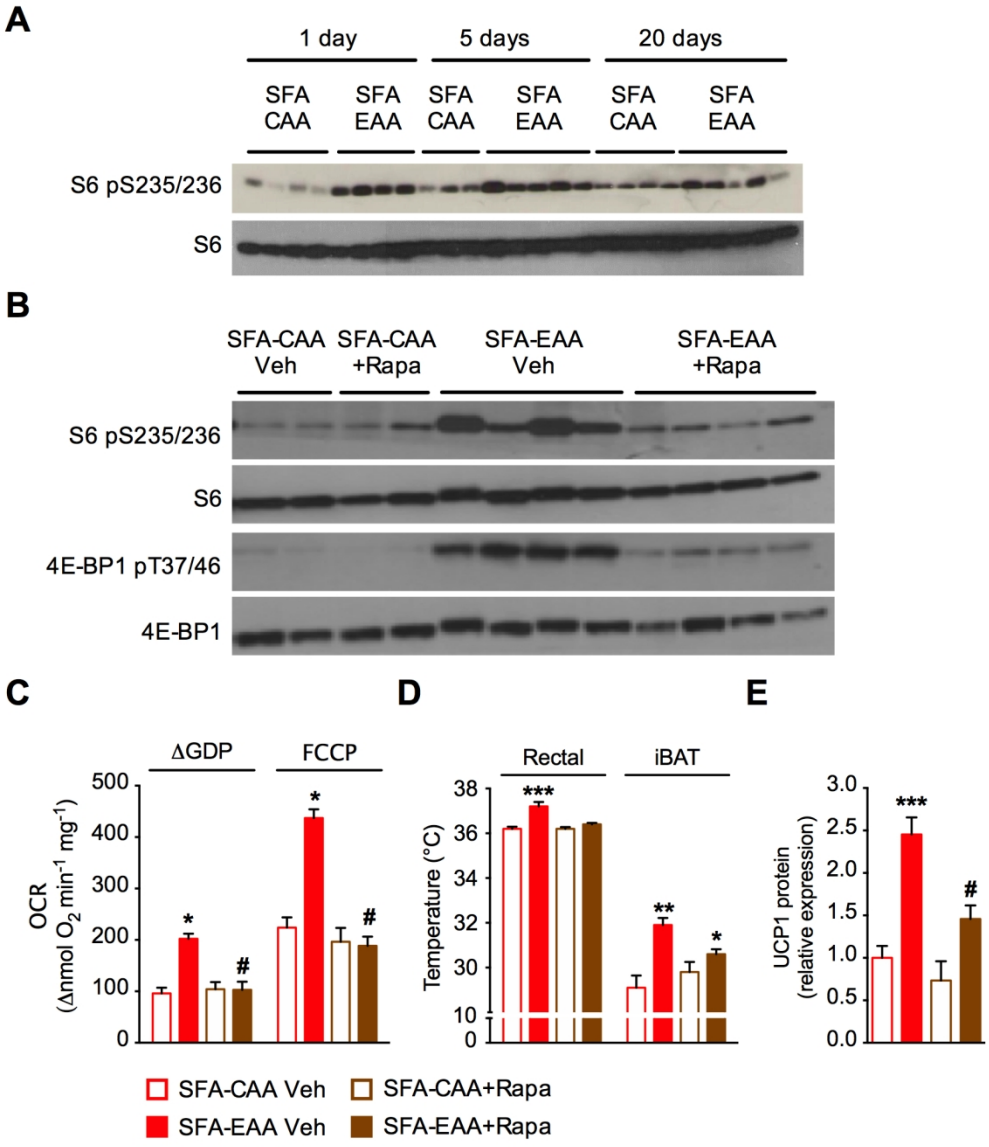

Figure 8

152x177mm (300 x 300 DPI)